Final Report
Microspoiler Actuation for Guided Projectiles

PI: Dr. Jonathan Rogers
Georgia Institute of Technology

Defense Advanced Research Projects Agency
(DARPA)
Tactical Technology Office (TTO)
DARPA Project: Microspoiler Actuation for Guided Projectiles
Purchase Requisition No. HR0011410748
Issued by DARPA/CMO under Contract No. HR0011-14-C-0126

A. Task Objectives

The goal of this project was to further mature microspoiler technology to the extent that it could be incorporated into current and future smart weapons designs. Several program objectives, including mechanical design and fabrication, trade study analysis, and limited flight experiments were defined as a collaborative effort between the Georgia Institute of Technology (Georgia Tech) and the Army Research Laboratory (ARL) for DARPA.

- **Objective 1: Perform Trade Studies to Optimize Microspoiler Configuration**
  Extensive trade studies will be performed for an example medium-caliber projectile (in the 30mm and/or 57mm class) to derive optimal microspoiler configurations (size, placement, number, and shape) in terms of maximum control authority and minimum power consumption. Example actively controlled trajectories will be simulated, including range-extension maneuvers to generate predictions of maneuver performance for several medium-caliber projectiles. Furthermore, control authority will be characterized at a variety of Mach numbers, including supersonic, transonic, and subsonic ranges.

- **Objective 2: Perform Studies on Scalability and Applicability to Spin-Stabilized Projectiles**
  Additional control authority trade studies will examine scalability of microspoiler performance to various calibers of fin-stabilized projectiles, including small, medium, and large calibers. These studies will yield general trends in how optimum configurations scale with projectile size. Further studies will examine microspoiler performance for an example spin-stabilized projectile, characterizing control authority performance and actuator bandwidth requirements. Finally, studies will be performed directly comparing control authority of microspoilers with canard mechanisms. These comparisons will quantify the increase in control authority of microspoilers over canards for the same drag penalty.

- **Objective 3: Design Microspoiler Actuator Mechanism**
  An active control mechanism will be designed to deploy and retract the microspoilers over the course of the projectile roll cycle for control purposes. The mechanism must be small and low-power, exhibit response times on the order of 10-100 Hz (or more, with exact requirements to be developed), and be hardened to gun-launch. Several alternative designs will be explored using various actuation techniques, and downselection to an optimal design will be performed through analysis of alternatives and a multivariable design criterion.

- **Objective 4: Construct Prototype Projectiles Equipped with Active Microspoiler Actuator Mechanism**
  A set of prototype medium-caliber fin-stabilized projectiles will be fabricated and equipped with the microspoiler actuator developed during Objective 3. These projectiles will be fabricated at a machine shop at the Georgia Institute of Technology. The fabrication process will make use of many of the machining methods and techniques already developed during previous microspoiler research.

- **Objective 5: Conduct Flight Experiment with Preprogrammed Maneuver Using Active Microspoiler-Equipped Projectile**
  Flight experiments will be conducted at the Army Research Lab using the active microspoiler-controlled projectiles fabricated in Objective 4. These flights will execute a preprogrammed maneuver that will validate the mechanical actuator design and provide data for aerodynamic characterization and control authority prediction. Results from these flight experiments are meant to enable potential transition of microspoiler technology and actuator design to current and future smart weapons programs.

B. Technical Problems

The potential benefits of guided projectile systems are well-known and include reduced collateral damage, increased weapon effectiveness, and greater standoff ranges. One of the main roadblocks in smart weapons technology development has been effective control actuation. Many current actuators suffer poor control authority, excessive power consumption, or overly complex design that reduces reliability. For future smart weapons development efforts to be successful, new actuator technologies are needed that provide reasonable control authority and reliability without undue cost or complexity.

The technical problems underlying this program involve aerodynamic prediction, aerodynamic optimization of the microspoiler mechanism, mechanical design/gun hardening, and parameter estimation from experimental data. These technical challenges were overcome successfully as described in Sections C, D, and E below.

C. General Methodology

The technical approach used to accomplish the stated objectives above included elements of simulation, mechanical design, and experimental test. The tools and methods employed throughout the program drew on simulation codes and experimental results developed during previous research on microspoiler actuation.

- **Technical Approach for Objective 1: Perform Trade Studies to Optimize Microspoiler Configuration**

  During Objective 1, extensive trade studies were performed to optimize microspoiler configuration in terms of size, placement, number of spoilers, and shape. These trade studies were conducted for the 30mm Army-Navy Finner. Control authority was evaluated for a given microspoiler configuration by measuring trajectory deflection and range extension using maximum control effort (i.e., microspoiler deployment over half of the roll cycle). These values were compared with baseline trajectories from an unguided round. Through computational fluid dynamics (CFD) trade studies in which all microspoiler parameters are varied in a systematic way, optimal configurations were identified. The

primary simulation tools used during this objective included steady CFD and a rigid body 6-degree-of-freedom rigid body dynamic model. Steady CFD simulations performed by ARL generated projectile aerodynamic coefficients with and without microspoilers extended. These aerodynamic parameters were used in subsequent 6DOF simulations of controlled trajectories to measure lateral acceleration performance for a given microspoiler configuration.

- **Technical Approach for Objective 2: Perform Studies on Applicability to Spin-Stabilized Projectiles**

  In this objective, use of microspoilers on spin-stabilized projectiles were explored. To accomplish this, similar steady CFD studies were performed with and without the presence of the aft fin set on the Army-Navy Finner. It was determined that about half of the control authority remained for the mechanism without the presence of the aft fins, indicating that the mechanism is applicable to spin-stabilized projectiles (although only about half as effective). These results are detailed further in Section D.

  Finally, a primary focus of this objective was to perform a direct quantitative comparison between microspoiler actuation and traditional canard actuation. Specifically, the advantages and disadvantages of microspoiler actuation and canard actuation were identified in terms of control authority. A microspoiler configuration and canard configuration were identified which produced the same zero-yaw drag penalty under maximum actuation (full canard deflection or maximum spoiler extension). Maximum divert trajectories were generated for the Army-Navy Finner using each of the actuator mechanisms, and control authority was compared. Given these direct numerical comparisons, the benefit of microspoiler actuation over canard actuation was quantified for equal drag penalty. These results are detailed further in the next section.

- **Technical Approach for Objective 3: Design Microspoiler Actuator Mechanism**

  Based on the optimal microspoiler configurations identified during Objective 1, an actuator mechanism was designed to extend and retract microspoilers in flight for the Army-Navy Finner. Several preliminary candidate mechanisms were designed in CAD using a variety of actuation approaches including linear solenoids and motor/cam designs. For each preliminary design, force and power requirements were estimated and components sized appropriately, including on-board batteries. All preliminary designs were evaluated from the perspective of actuation bandwidth, power requirements, manufacturability, and robustness to launch loads. A final actuator concept was downselected during this process, and prototypes were fabricated to verify operation of the design and manufacturing effort required. These prototypes were fabricated at the Georgia Tech Mechanical Engineering machine shop. A detailed description of the selected actuator concept is provided in Section F.

- **Technical Approach for Objective 4: Construct Prototype Projectiles Equipped with Active Microspoiler Actuator Mechanism**

  A set of integrated test projectiles was fabricated at the Georgia Institute of Technology Mechanical Engineering machine shop. Georgia Tech fabricated the projectiles according to a detailed specification of the Army-Navy Finner (30mm). Projectile manufacturing methods drew on existing techniques developed during previous microspoiler research efforts. A set of projectiles was machined with space for actuator installation, as well as a set of baseline projectiles without the actuator mechanism. Following projectile fabrication, a set of microspoiler actuators was manufactured and installed in the test projectiles, along with required electronics and batteries.

Actuation performance of each projectile at the appropriate frequency was verified in benchtop experiments to characterize rise time and steady state oscillation rates. Fabrication of projectiles and mechanical components made use of computer numerically controlled (CNC) mills and lathes as well as wire electrical-discharge machine (EDM) and EDM sync machines as needed.

Prior to manufacture of the entire set of test articles, the first integrated projectile was tested on a high velocity acceleration shock test machine at the Army Research Laboratory. This ensured launch survivability of the design.

Electronics were fabricated at Georgia Tech in the electronics shop area of the Intelligent Robotics and Emergent Automation Laboratory, a robotics facility run by the PI. Electronics packages were then incorporated into the test projectiles and shock-tested with the first prototype along with the maneuver mechanism as described above.

- **Technical Approach for Objective 5: Conduct Flight Experiment with Preprogrammed Maneuver using Active Microspoiler-Equipped Projectile**

The test projectiles fabricated during Objective 4 were fired at the Army Research Laboratory's Transonic spark range in Aberdeen, Md., in November-December 2015. The goals of the test were to
1) demonstrate actuation of the microspoilers at or near the roll frequency of the test projectile, and 2) to acquire experimental flight data for characterization of control authority with time-varying actuation of the microspoiler mechanism. Both baseline (unactuated) and actively-controlled projectiles were fired for comparison purposes. A total of 19 shots were conducted (6 non-active, 13 active).

The actively-controlled test projectiles completed a preprogrammed maneuver and thus required no feedback. The preprogrammed maneuver was designed such that sufficient aerodynamic motion was induced but the projectile remained within the confines of the test range. Specifically, the microspoilers were actuated just off the projectile spin rate yielding a coning motion with very little net divert.

Spark range testing was performed by ARL personnel in accordance with standard ARL procedures. Following the tests, spark range data was reduced by ARL technicians. Georgia Tech is currently processing the aerodynamic data for the purposes of updated parameter estimation. All aerodynamic coefficient estimation is being performed using the Projectile Aerodynamic Model Estimation (PACE) tool developed by Montalvo and Costello, which is based on standard maximum likelihood methods. These results are expected to be available in March 2016.

D. Technical Results

<u>Microspoiler Configuration Optimization</u>

Prior work has demonstrated that the microspoiler mechanism is an effective method to generate control authority for smart weapons. A primary goal of this program is to increase control authority of the mechanism by optimizing the microspoiler configuration (arrangement, size, shape, height, and placement on the projectile). Computational fluid dynamics must be employed to determine aerodynamic coefficients for a projectile equipped with a given set of microspoilers. However, the very large number

of configuration variables, coupled with the long runtimes of typical CFD analysis codes, means that an exhaustive search of the design space is not feasible.

For this reason, the approach taken during this program is to identify several key points in the design space and analyze performance at these points using static CFD. Based on these results, the key factors driving control authority can be established, and additional design changes can be made to incrementally improve performance. This process continues until it is determined that further design changes will not result in noticeable improvements.

Given this methodology, Dr. Jubaraj Sahu of the Army Research Laboratory initiated eight static CFD runs, four with six microspoilers and four with eight microspoilers. In each run, the microspoilers were arranged differently on the projectile, including in a backwards-V and forwards-V configuration. Static CFD was performed at Mach 2.5 with zero angle of attack using a 30mm Army Navy Finner projectile. For each case the axial drag, normal force, and pitching moment were calculated. Computed surface pressure contours for each case are shown in Figure 1, with the six-spoiler cases shown on the left and the eight-spoiler cases shown on the right. Table 1 shows the computed forces and moments for each case.

Figure 1 shows some interesting phenomena. First, note the complexity of the flowfields which makes any analytical solution to this problem essentially infeasible. Second, note the interacting shockwaves which yield successive regions of high and low pressure upstream and downstream of the spoiler respectively. For the top three cases, the region behind the aft set of the spoilers exhibits particularly low surface pressures. After examining these six cases, the bottom two cases were generated, in which the aft set of spoilers is placed exactly at the rear of the projectile. This alleviates the low-pressure region, which improves control authority substantially. As shown in Table 1, the V-configuration of the spoilers (Cases 4 and 8) generates highest control authority, and placement of the aft row of spoilers as close as possible to the rear of the projectile yields even higher control authority at negligible additional drag penalty.

A final study was been performed to examine the effects of increasing spoiler heights from the front of the projectile to the back. In this study, the first row of spoilers had the same height as those shown in Figure 1, and height was increased linearly such that the rear row of spoilers was twice as high as the first. This configuration resulted in about a 40% increase in control authority, but yielded about twice as much drag. For this reason, the current optimized spoiler design is judged to be the eight-spoiler V-configuration with uniform height as shown at the bottom right of Figure 1, labeled Case 8 in Table 1. **Note that this optimal configuration yields 50% more control authority than the microspoiler configurations studied in prior experiments (labeled as Case 0 in Table 1), with only a 35% increase in drag. This 50% increase in control authority represents a significant advancement and was a major goal of this program.**

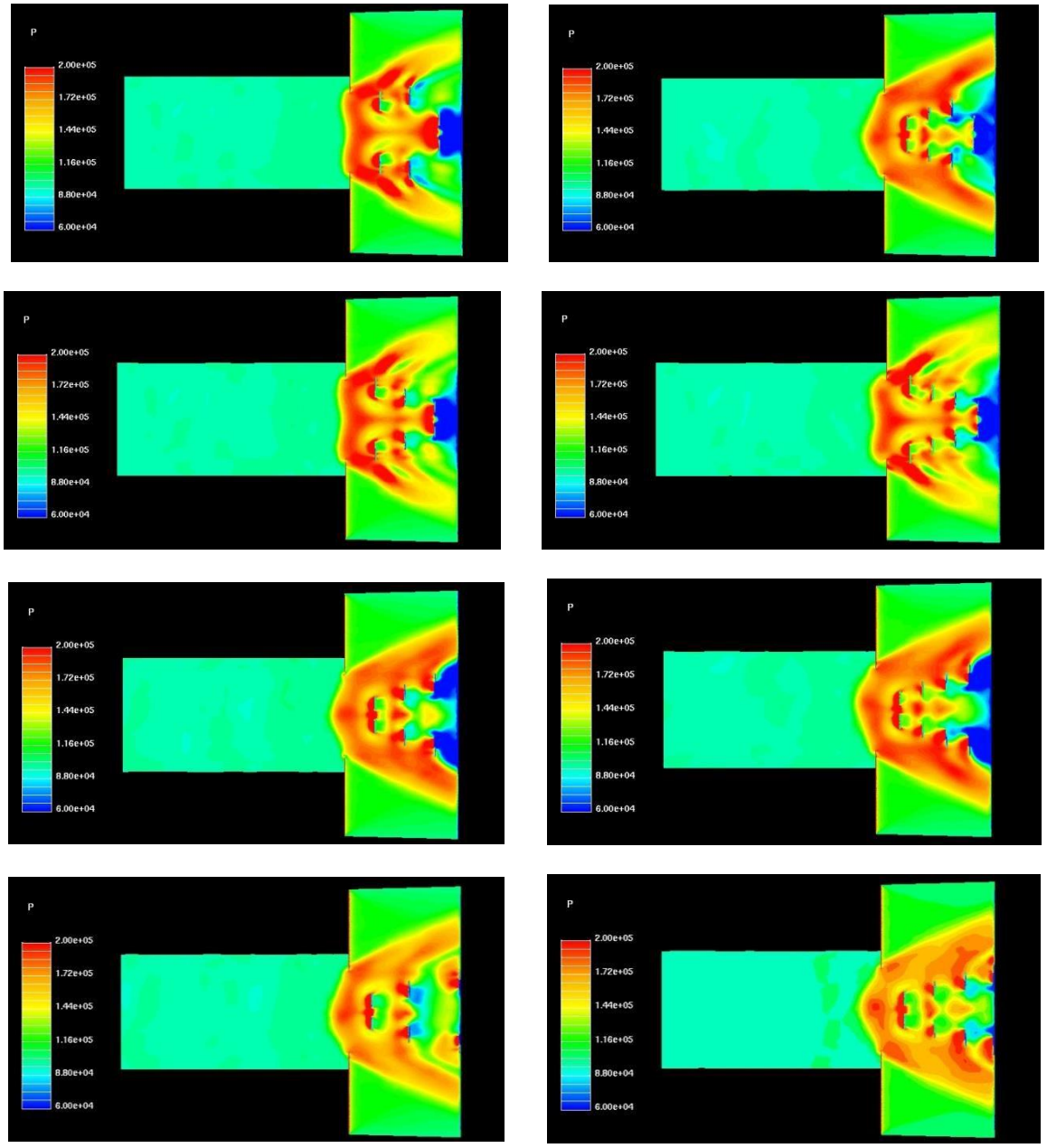

Figure 1. Computed surface pressure contours in the afterbody fin region near the microflaps, $M = 2.5$, $\alpha = 0°$, left column is six-flaps cases, right column is eight-flaps cases. Cases 1-4 are shown top to bottom in the left column, Cases 5-8 are shown top to bottom in the right column.

Table 1. Computed Delta Forces and Moments Due to Microspoilers, $M = 2.5$, $\alpha = 0°$.

Cases	Delta Normal Force δF_z, (N)	Delta Pitching Moment δM_y, (N-m)	Delta Axial Force (N)
Case 0 (4 flaps) (Used in prior work)	-40.0	4.20	17.0
Case 1 (6 flaps)	-47.5	5.87	19.9
Case 2 (6 flaps)	-50.2	6.23	20.0
Case 3 (6 flaps)	-50.8	6.34	21.2
Case 4 (6 flaps)	-55.2	6.93	21.6
Case 5 (8 flaps)	-51.4	6.25	20.2
Case 6 (8 flaps)	-52.5	6.34	21.6
Case 7 (8 flaps)	-55.5	6.8	23.1
Case 8 (8 flaps)	-60.6	7.56	23.6

Control Authority Characterization

To determine the end result of this configuration optimization in terms of control authority, trajectory simulation studies were performed using the steady microspoiler loads computed by static CFD as shown in Table 1. Assuming four sets of microspoilers (one set between each pair of fins) and a 90-degree activation window, a projectile trajectory was simulated without gravity at zero quadrant elevation. The 30mm Army Navy Finner projectile was used with a static margin slightly reduced from the nominal value (by about 0.93 calibers). Maximum control was commanded in the left crossrange direction, and the simulation was terminated at 1000m downrange. One simulation was performed for each of the eight cases listed in Table 1, as well as a baseline case without the microspoilers for comparison.

Figures 2-6 show the results of this trade study. First, note in Figure 2 that the optimized microspoiler case (Case 8) shows a maximum deflection of about 100m, compared to about 53m for Case 0 (the four-spoiler configuration used in previous work). Figure 3 shows that the optimized spoiler case achieves almost 5 deg steady-state angle of attack, with the other cases exhibiting between 2 and 4 deg. Figures 4 and 5 show roll rate and yaw angle time histories respectively. In Figure 6, it can be seen that increased control authority results in increased drag, although the impact velocity for Case 8 is only about 2% lower than the impact velocity for the baseline projectile with no spoilers.

Overall, these results demonstrate that the optimization process employed during this program has improved control authority by almost two times over the original microspoiler configuration that was previously studied. Table 2 lists the average lateral acceleration generated by the microspoiler mechanisms. **Note that the optimized configuration, Case 8, generates almost 18 gs of average lateral acceleration over this 1-km flight.** This is a significant improvement over Case 0, and can be improved further by reducing the static stability of the projectile.

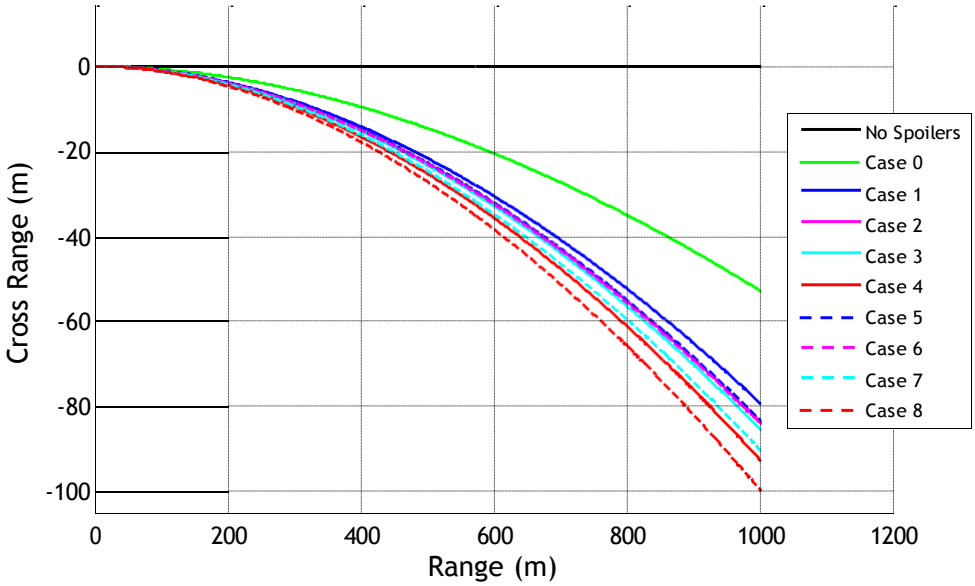

Figure 2. Crossrange vs Range for Example Simulations.

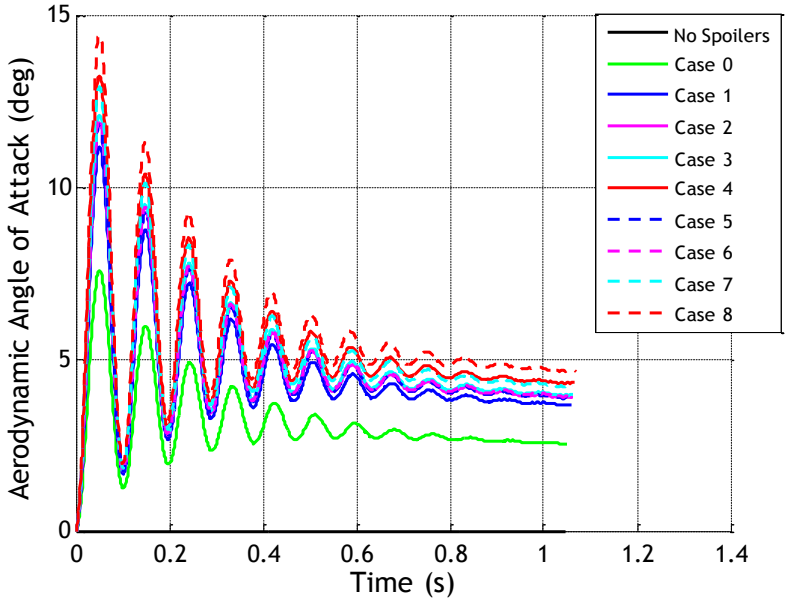

Figure 3. Total Angle of Attack vs Time for Example Simulations.

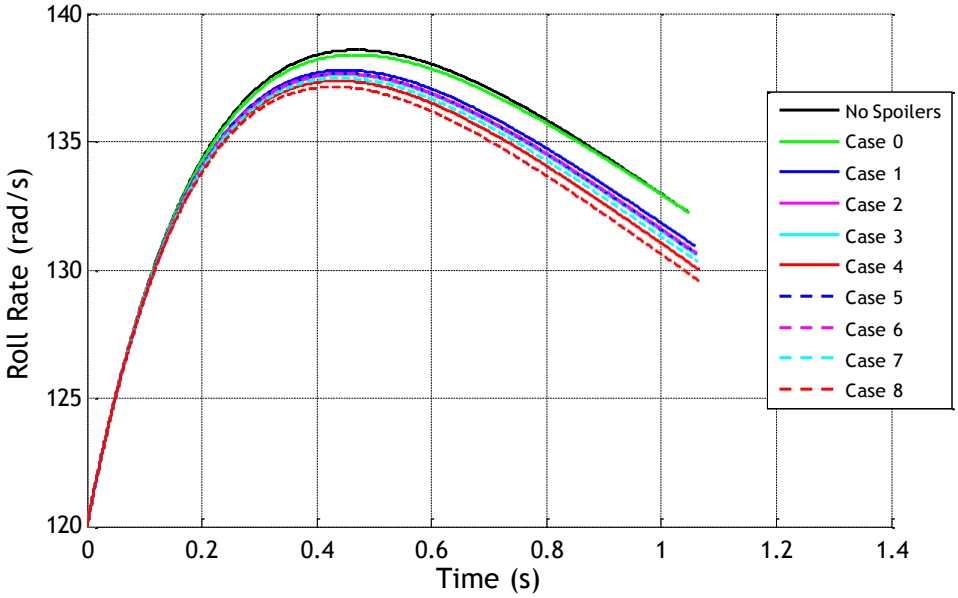

Figure 4. Roll Rate vs Time for Example Simulations.

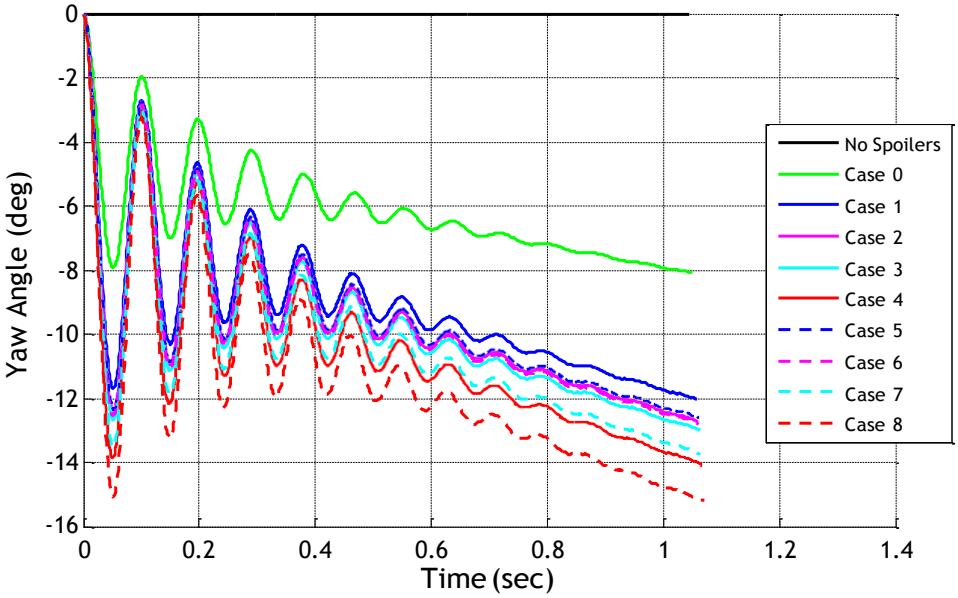

Figure 5. Yaw Angle vs Time for Example Simulations.

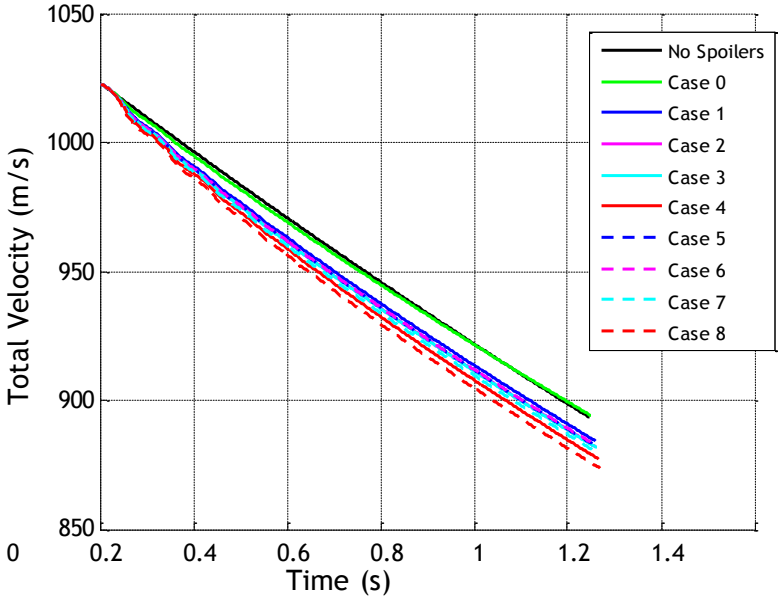

Figure 6. Total Velocity vs Time for Example Simulations.

Table 2. Average Lateral Acceleration for Example Simulations.

Case	Average Lateral Acceleration (g's)
0	9.78
1	14.4
2	15.2
3	15.5
4	16.7
5	15.1
6	15.2
7	16.3
8	17.8

Microspoiler Performance Mach Number Trade Study

One of the main objectives of this program is to characterize control authority of microspoilers across the entire Mach number range for fin-stabilized projectiles. This requires aerodynamic prediction of forces and moments due to the mechanism from subsonic (Mach 0.8) to high supersonic speeds (Mach 5). Dr. Jubaraj Sahu of the Army Research Laboratory completed this aerodynamic prediction using established steady-state CFD tools.

Table 2 shows the integrated forces and moments, measured with respect to the standard 30mm Army-Navy Finner, due to the presence of the optimized eight-microspoiler configuration. This data is also

plotted in Figure 7, where it is compared with the previous four-spoiler geometry. Note the general trend that control forces and moments, as well as drag, increase as a function of Mach number as expected due to the higher dynamic pressure on the upwind side of the spoiler surface. However, an interesting trend is evident in the subsonic regime. For the optimized eight-spoiler geometry, the pitching moment induced by the mechanism remains largely constant at about 1.5 N-m from Mach 0.8 through Mach 1.1. This is in contrast with the prior four-spoiler design, which yields approximately zero pitching moment in this subsonic/transonic regime. Thus, it is clear that the new optimized eight-spoiler geometry maintains some control effectiveness even in subsonic flight.

To translate this aerodynamic data into lateral acceleration performance, trajectory simulations were performed using the aerodynamic parameters in Table 2. Projectile trajectories were simulated without gravity at zero gun elevation. The standard 30mm Army-Navy Finner was used with maximum control commanded in the left crossrange direction. Simulations were performed from Mach 0.8 to Mach 3.75. Figures 8-10 show the results of these simulations. Figure 8 clearly shows that greater lateral deflection is exhibited as Mach number increases. Figure 9 reinforces this trend by showing higher steady-state angles of attack induced by the microspoilers at higher Mach numbers. Finally, Figure 10 shows that average lateral acceleration induced by the microspoiler mechanism increases approximately exponentially with Mach number.

An interesting trend is evident at lower Mach numbers in the range of Mach 0.8-1.2. As shown in Figure 7, while control moment generally decreases approximately linearly with Mach number, at about Mach 1.1 it levels off and remains constant within the range Mach 0.8-1.1. This yields similar values for lateral acceleration in this range as shown in Figure 4. As a result, total deflection is actually greater for Mach 0.8 than for Mach 1.25, since they each have nearly equal lateral acceleration but the Mach 0.8 projectile travels slower. This trend is shown in Figure 8, where deflection decreases at first from Mach 0.8 and 1.25, then begins to increase as Mach number grows.

Several important conclusions arise from these CFD and trajectory prediction results. First, the microspoiler geometry has now been successfully optimized and comparisons between the optimized geometry and the original spoiler geometry show very significant control increase at little drag penalty. Second, lateral maneuver authority with the optimized eight-spoiler geometry grows exponentially with respect to Mach number. While maneuver performance is lower in the subsonic regime, some control authority is still maintained. Overall, results from this study show that the microspoiler mechanism is a viable control actuator for projectiles at high subsonic and supersonic flight speeds, and that the geometry optimization efforts pursued during this program were extremely successful.

The data in Table 2 and Figures 7-10 represent the final results set for microspoiler control authority prediction for fin-stabilized projectiles covering the entire Mach number range.

Table 2. Computed Delta Forces and Moments Due to Microspoilers, 30mm Army-Navy Finner with 8-Spoiler Geometry.

Mach Number	Delta Normal Force δF_z, (N)	Delta Pitching Moment δM_y, (N-m)	Delta Axial Force (N)
0.80	-10.9	1.23	3.7
0.90	-12.8	1.44	5.1
0.92	-12.8	1.44	5.4
0.95	-12.6	1.40	5.8
0.98	-11.8	1.30	6.3
1.1	-13.7	1.51	7.7
1.5	-34.4	4.13	13.1
2.0	-47.8	5.92	18.5
2.5	-60.6	7.56	23.7
3.0	-73.7	9.25	29.0
4.0	-103.9	13.05	43.1
5.0	-135.2	17.00	59.2

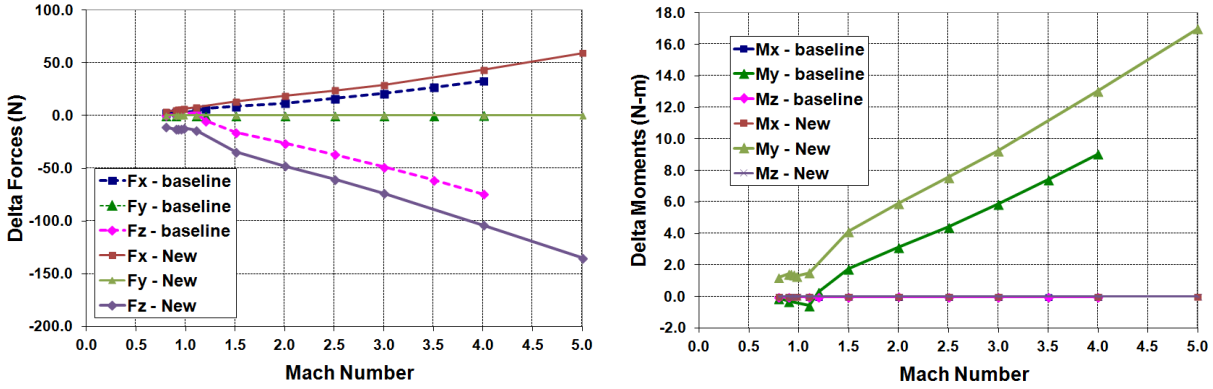

Figure 7. Delta Forces and Moments Due to Four-Spoiler "Baseline" Configuration and Eight-Spoiler "New" [Optimized] Configuration.

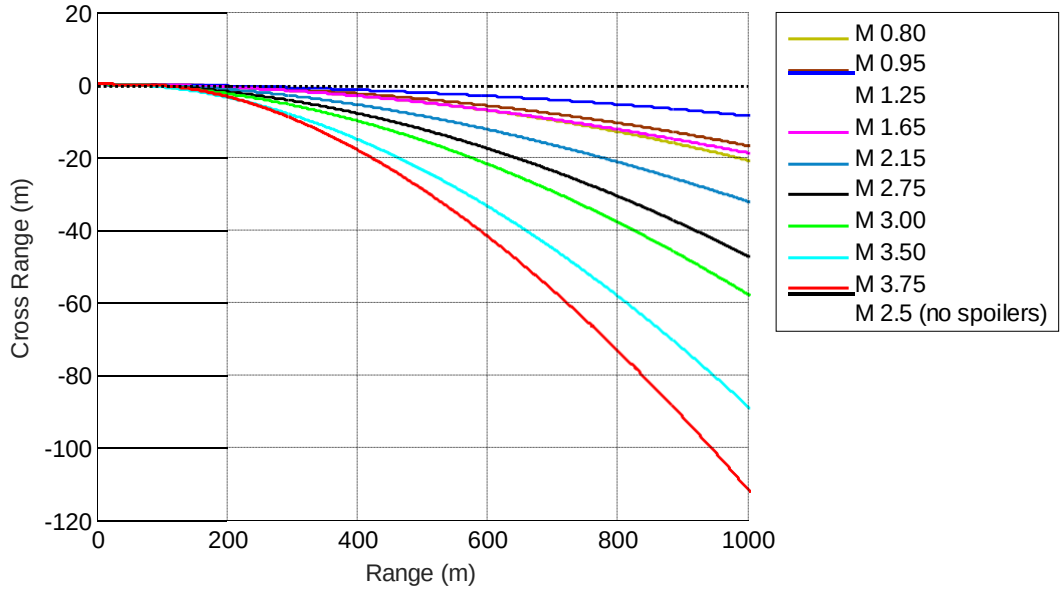

Figure 8. Cross Range vs Range for Example Microspoiler Trajectories, Varying Muzzle Velocity.

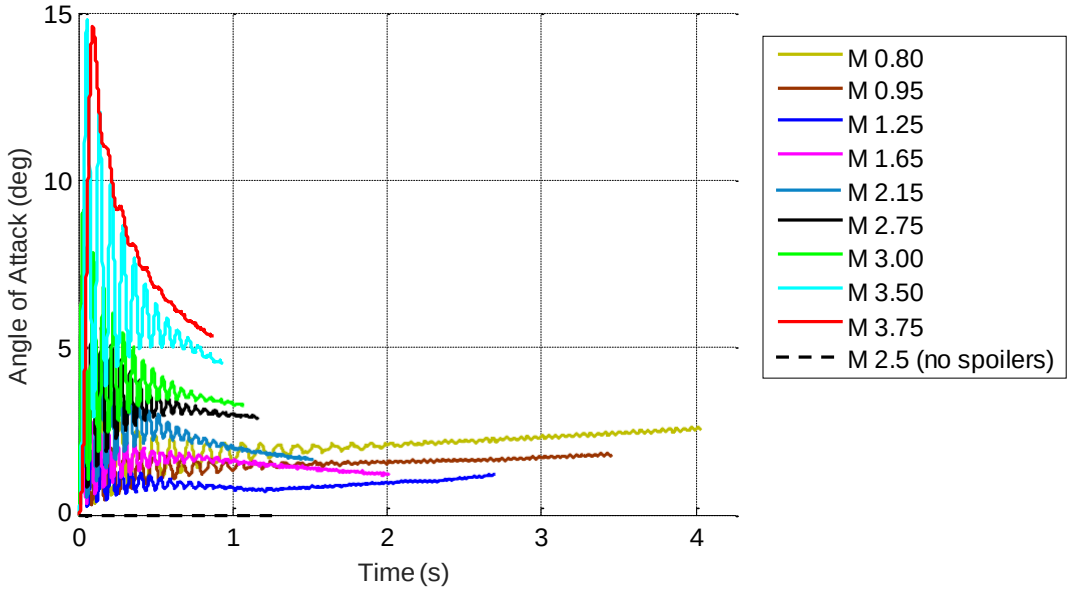

Figure 9. Angle of Attack vs Time for Example Microspoiler Trajectories, Varying Muzzle Velocity.

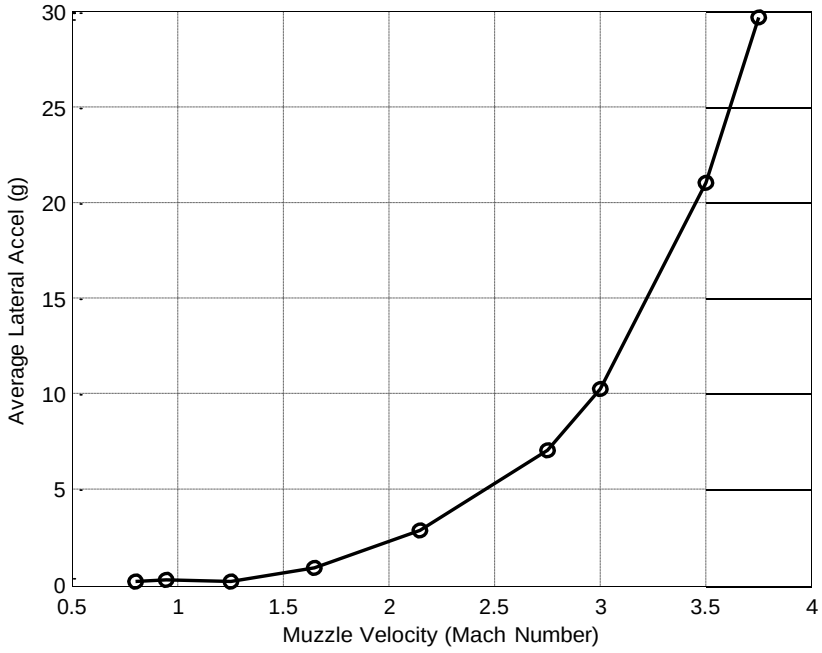

Figure 10. Average Lateral Acceleration vs Launch Velocity for Example Microspoiler Trajectories.

Microspoiler Performance on Spin-Stabilized Projectiles

One objective of this program is to study the effectiveness of the microspoiler mechanism on spin-stabilized rounds. The key difference between spinners and finners is the absence of the rear fin set, which acts to amplify the effect of the microspoilers. Shock waves shed from the microspoilers in supersonic flight impinge on the rear fin set, amplifying the aerodynamic asymmetry and the resulting control authority. To quantify the amplification caused by the fins, static CFD tests were performed with and without fins being present on the body, and aerodynamic forces and moments computed. The optimal eight-spoiler configuration discussed in previous progress reports was used for these studies. The results of this comparison are shown in Figures 11 and 12, as well as in Table 3. In Figure 11, it is clear that the control moment in the no-fin case is approximately half of that in the finned case, signifying that control authority on a spin-stabilized round will be about half of that on a fin-stabilized round. In Figure 12, performance in the no-fin case is compared with the four-spoiler geometry that was used in previous development studies (baseline) prior to the optimization process performed under this program. In Figure 12, it is clear that the control authority on the spin-stabilized round is relatively close to that of the four-spoiler fin-stabilized case.

Overall, these results show that the mechanism still retains considerable control authority for spin-stabilized rounds and thus remains a viable control mechanism for this class of munitions. Lateral acceleration capability for the spin-stabilized case is judged to be about half that of finners. Note however the complete loss of control authority at subsonic speeds in the no-fin case (which can be seen in Figure 11). Thus, the mechanism will only be effective for spinners at Mach numbers well above 1.

Table 3. Computed Delta Forces and Moments Due to Microspoilers, 30mm Army-Navy Finner with 8-Spoiler Geometry.

Mach Number	Normal Force (Finned), N	Normal Force (No-Fin), N	Pitching Moment (Finned), N-m	Pitching Moment (No-Fin), N-m	Axial Force (Finned), N	Axial Force (No-Fin), N
0.80	-10.9	-2.19	1.23	0.23	3.7	1.5
0.90	-12.8	-2.74	1.44	0.30	5.1	2.4
0.92	-12.8	-2.90	1.44	0.31	5.4	2.6
0.95	-12.6	-2.94	1.40	0.32	5.8	3.0
0.98	-11.8	-2.74	1.30	0.30	6.3	3.6
1.1	-13.7	-2.89	1.51	0.33	7.7	4.7
1.5	-34.4	-9.11	4.13	1.14	13.1	8.5
2.0	-47.8	-16.53	5.92	2.12	18.5	14.1
2.5	-60.6	-24.32	7.56	3.13	23.7	19.9
3.0	-73.7	-32.53	9.25	4.20	29.0	23.7
4.0	-103.9	-50.92	13.05	6.56	43.1	37.9
5.0	-135.2	-71.27	17.00	9.18	59.2	52.8

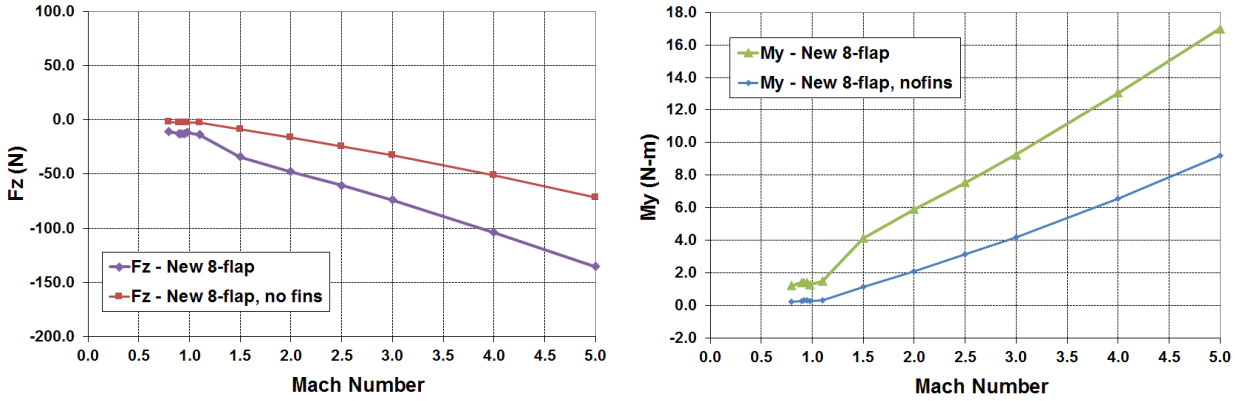

Figure 11. Normal Force and Pitching Moment Generated by Microspoilers vs Mach Number, Finned and No-Fin Configurations.

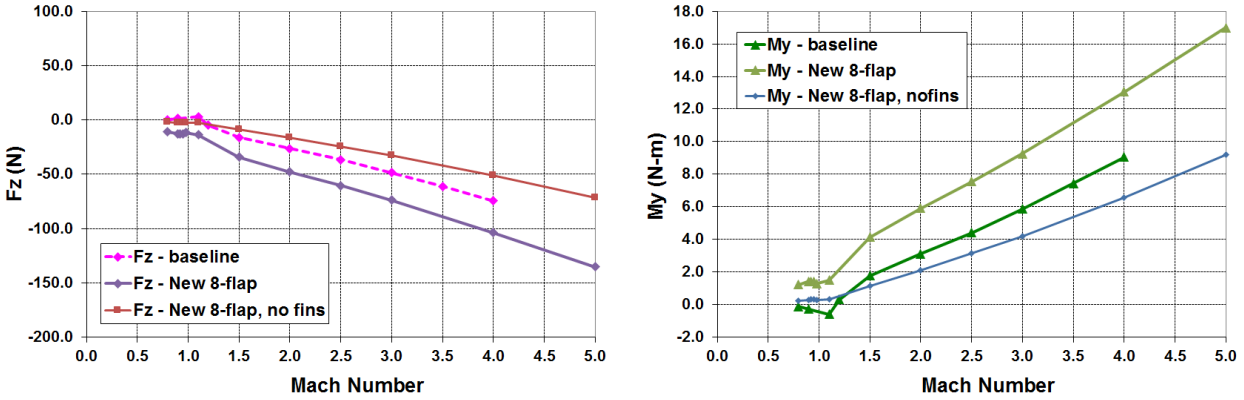

Figure 12. Normal Force and Pitching Moment Generated by Microspoilers vs Mach Number Compared to Baseline Four-Spoiler Geometry.

Projectile Flight Experiments at the Army Research Laboratory

A series of projectile flight tests were carried out at ARL using the prototype designs described in Section F. These tests were conducted during the third week of November (outdoor) and third week of December (indoor). A picture of one of the test articles is shown in Figure 13. In total, two active and two baseline projectiles were fired outdoors to ensure proper sabot separation and stable flight. These tests proceeded without incident and the projectiles were deemed to be suitable for indoor testing. Four baseline and 11 active projectiles were fired in the Transonic Spark Range on December 21-22, yielding spark range shadowgraphs and high speed video for each flight. ARL provided Georgia Tech with estimated position and orientation at each spark station derived from the shadowgraphs. An example shadowgraph is shown in Figure 14, while plots of pitch and yaw angle vs down range location are shown in Figures 15 and 16 respectively.

In Figure 15, the difference in angular motion between active and baseline rounds can be clearly seen. This indicates that the actuator did in fact operate as desired and induced a reasonable level of angular motion suitable for system identification. The reason that a clear difference between active and baseline performance is seen in Figure 15, but not in Figure 16, is because the rounds were loaded in the barrel in identical roll positions for each shot. The position and orientation data provided by ARL is currently being used by Georgia Tech to perform aerodynamic parameter estimation (to be completed February 2016). The result of this parameter estimation process is expected to be an updated, experimentally validated set of aerodynamic coefficients for the microspoiler mechanism. These will be extremely useful in updated predictions of control authority and actuator efficacy.

Figure 13. Test Article (active projectile) Used in Outdoor Flight Experiments.

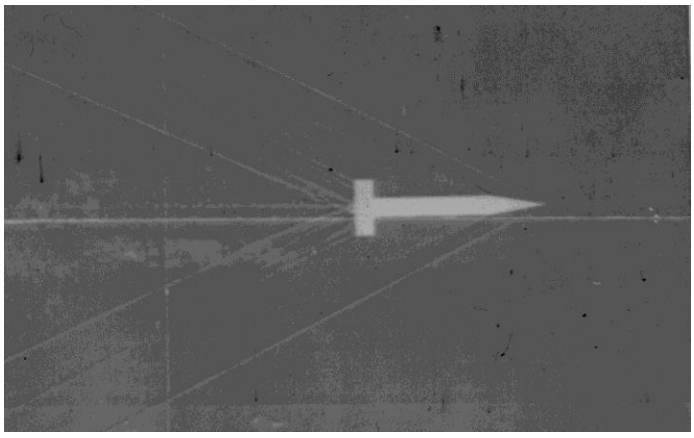

Figure 14. Example Spark Range Shadowgraph from Microspoiler Flight Experiments.

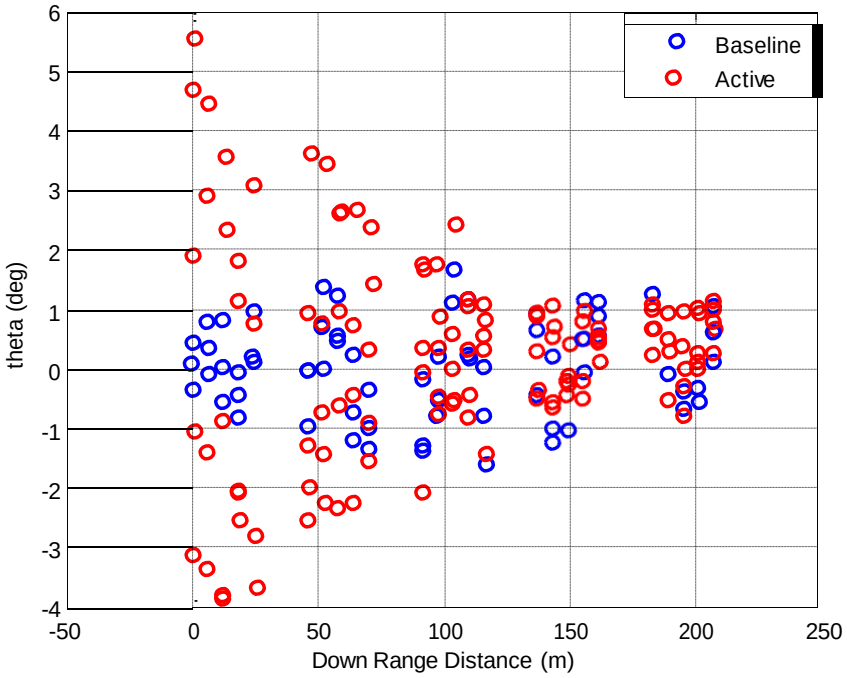

Figure 15. Pitch Angle vs Down Range Distance for Microspoiler Flight Experiments.

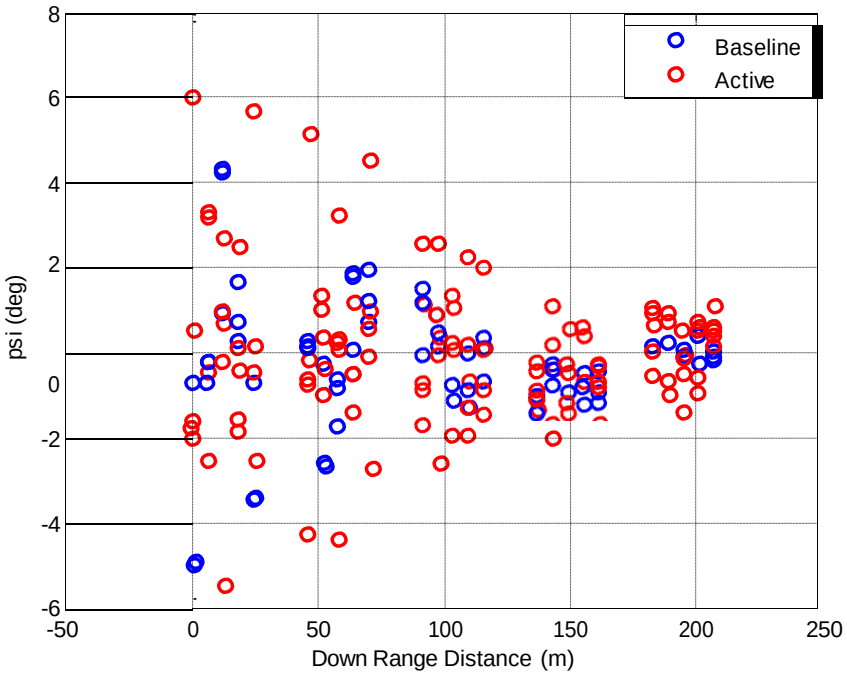

Figure 16. Yaw Angle vs Down Range Distance for Microspoiler Flight Experiments.

E. Important Findings and Conclusions

The important findings and conclusions of this work are detailed in Section D above and summarized here. From the analytical aerodynamic studies, the following findings were established:

- **Configuration Optimization:** The inverted "V" shape shown in Figure 1, Case 8 provides the maximum control authority for the microspoiler mechanism. The last row of spoilers should generally be located at the rear edge of the projectile to preclude the low-pressure region behind the last row of spoilers from impacting the projectile. Generally, more spoilers result in increased control authority, although no testing was performed with spoiler numbers greater than eight (for a single set). An optimal height exists for a given size/geometry which achieves the best balance of control authority and resulting drag penalty.

- **Mach Scalability:** As shown in Figure 10, the microspoiler mechanism becomes exponentially more effective as Mach number increases. This has significant implications for high Mach/hypersonic projectiles, which are expected to be able to leverage this actuator mechanism extremely effectively. As shown in Figure 10, some control authority is maintained at subsonic speeds, although it is greatly diminished.

- **Applicability to Spin-Stabilized Projectiles:** Microspoilers are about half as effective in the absence of fins are they are when fins are present. Thus, they should still retain a reasonable amount of control authority for spin-stabilized projectiles, especially at high Mach numbers. It was noted in Figures 11-12 that control authority at subsonic speeds in the absence of fins is reduced to almost zero.

- **Comparison to Canards:** Microspoilers offer roughly equivalent maneuver performance to canard actuators in terms of lateral divert capability vs. drag penalty. However, spoilers are a lot simpler to implement mechanically and may thus offer a very viable and important alternative to canards. Furthermore, the combination of canards and microspoilers implemented on the same projectile may offer a very powerful actuator solution, as spoilers may be used to effect control at high Mach numbers while canards can take over at low Mach numbers. Simulation studies with both actuators showed that control authority using both mechanisms was essentially additive.

- **Mechanical Implementation:** Experimental studies conducted during this program showed that active microspoilers can be feasibly implemented and gun-hardened for medium-caliber rounds. The mechanical design of such systems can leverage cam mechanisms coupled to a motor and a simple electronics package.

F. Significant Hardware Development

A significant hardware development effort was pursued during this program to design and construct flight test articles with the active microspoiler mechanism. This section details this process and the final mechanical design.

Flight testing of the microspoiler-equipped projectile was accomplished using a 30mm Army-Navy Finner projectile equipped with a single set of eight microspoilers (of the optimized configuration) between a single set of fins. The initial stage of test preparation involved selecting three critical projectile

design parameters: fin cant, mass center placement, and spoiler actuation frequency. The goal of these tests was to generate enough control excitation with the spoilers so that precise spark range measurements could be made and aerodynamic coefficients could be estimated. However, too much control excitation is problematic since the projectile must remain within the viewing windows of the spark stations (approximately 2 m x 2 m), and more importantly within the confines of the spark range itself. To accomplish this, the microspoiler actuation frequency was different from the projectile roll frequency such that control moments are integrated out over a roll cycle and are not biased in a single direction. The resulting flight path exhibited measurable angle of attack perturbations without significant cross-range deviation. The parameters chosen for this flight experiment were a 1.25 deg fin cant, 70 Hz microspoiler actuation frequency, and 450mm stationline CG position measured from the base. These parameters were chosen through large-scale trade studies using 6DOF simulation and are detailed in an earlier progress report.

Given the spoiler actuation frequency of 70 Hz, a motor-cam actuator was designed for the 30mm Army-Navy Finner based on a positive return mechanism. The advantage of the positive return mechanism is that it yields an approximately 90-deg activation window, which is optimal in terms of control performance. CAD drawings of this mechanism are shown in Figures 17 and 18. As seen in these figures, four spoiler plates are embedded within the fin set of the projectile, with two spoilers attached to each plate. Rotational motion of the cam forces the spoiler plates into the desired linear, oscillatory motion.

Figures 19-21 show CAD drawings of the integrated projectile. Note that the spoilers and associated positive return mechanism occupy the rear of the projectile, with the motor and battery packs stacked farther forward. Further note the presence of a spin pin protruding from the aft end of the projectile – during interpretation of spark range shadowgraphs this assists in identifying projectile orientation. While not explicitly shown in the CAD drawings, the entire interior of the round (except of course the aft spoiler section) was potted so that there was no empty space. This is critical for launch survivability by ensuring that components do not shift or break during launch acceleration.

In April 2015, shock table experiments were performed at ARL to determine a suitable motor for use during these flight experiments. Four motors were shock tested to a maximum load of 23,000 gs – two brushless DC motors and two brushed DC motors. All motors were of reasonably high quality and were meant for precision applications. Surprisingly, only one of these motors survived the shock table experiments with no damage. This motor was the Maxon A-Max 110147 brushed motor, shown in Figure 22. This motor was further shock tested up to 26,800 gs and again survived with no damage. Overall, these test signify that the motor was capable of surviving gun launch up to Mach 2.5 and thus it was selected as the motor to be used during these flight tests.

An electronic mechanism must also be incorporated into the round to activate the spoiler mechanism at gun launch. A latch activation circuit was designed for this purpose. The latch circuit is constructed by combining two MOSFET transistors with a shock switch, such that when the shock switch is activated, the motor circuit latches on (permanently). Thus, momentary closure of the shock switch during gun launch will activate the motor for the remainder of the flight. The shock sensor selected for use is the SignalQuest SQ-ASE series, rated to switch at 4,000 gs (and previously used by ARL successfully for this purpose). Note that this high-g activation level is selected so that the circuit will not activate accidentally during transport. The activation circuitboard was integrated so that it was directly attached to the motor, as shown in Figure 23. Also highlighted in Figure 23 is the SignalQuest shock sensor. Figure 24 shows the latch circuit schematic used for this project.

Given completion of these component designs, Georgia Tech began prototyping completely integrated

projectiles equipped with the fully functional spoiler mechanism. The projectile was constructed of stainless steel and aluminum in three parts which attach together. Figure 25 shows a fully constructed prototype, while Figure 26 shows the spoiler section in more detail. Note that the spoiler section is designed in multiple pieces so that it can be easily assembled and integrated with the main projectile body. This is shown in Figure 27.

During flight experiments, the projectile was launched from a 120mm gun tube and thus required a sabot. Figure 28 shows a CAD drawing of the projectile integrated with the sabot, consisting of the petals surrounding the projectile, base plate, and obdurator. In addition to the projectile manufacturing activities above, Georgia Tech fabricated the nylon sabots as shown in Figure 28.

In total, Georgia Tech manufactured over 30 sabots and approximately 25 projectiles (10 baseline, 15 active). Each projectile and sabot combination was produced at an approximate cost of $1,000 per round. Shock table tests and flight experiments confirmed the ability of the projectile to survive gun launch and deploy the actuator in an oscillatory fashion successfully.

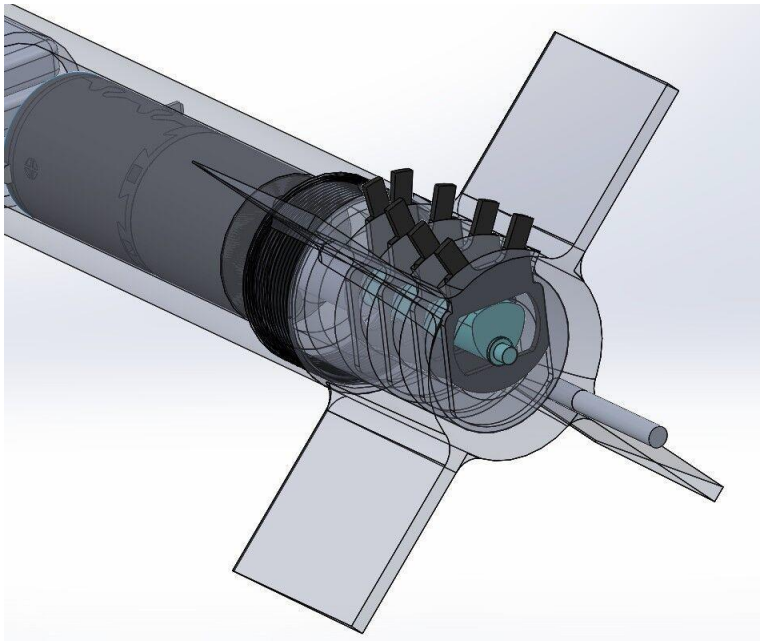

Figure 17. Motor-Cam Positive Return Mechanism Which Drives Microspoiler Actuation.

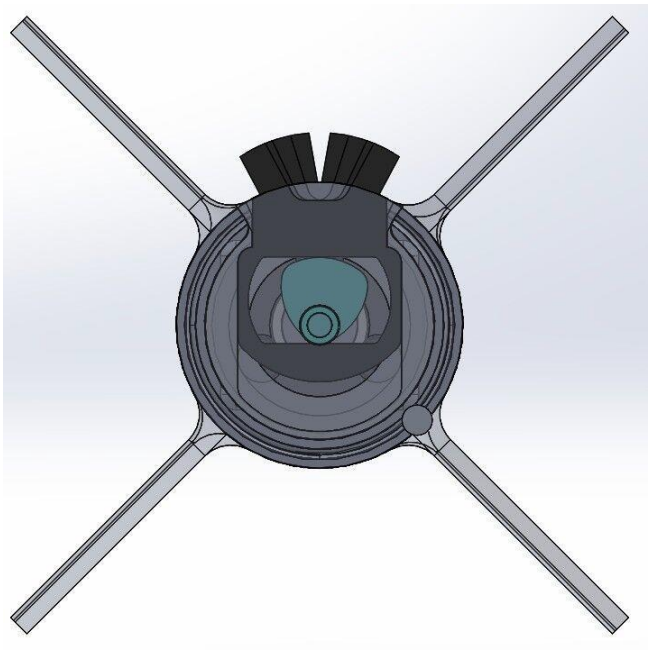

Figure 18. Rear View of Motor-Cam Positive Return Mechanism. Note Reuleaux triangular cam which is unique to positive return mechanism. This generates a ~90-deg activation window of the spoiler mechanism.

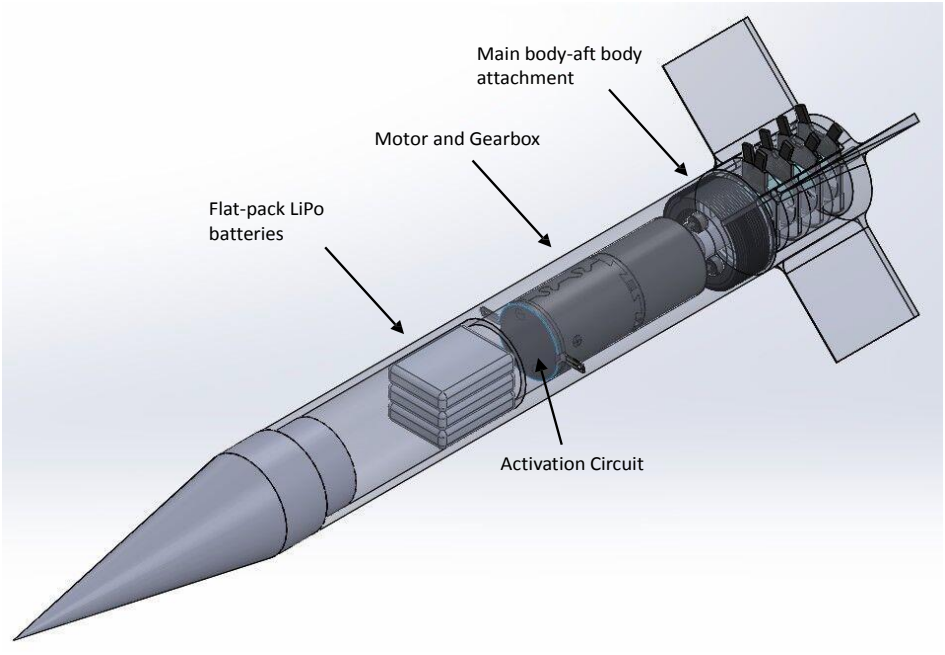

Figure 19. CAD Drawing of Integrated Projectile.

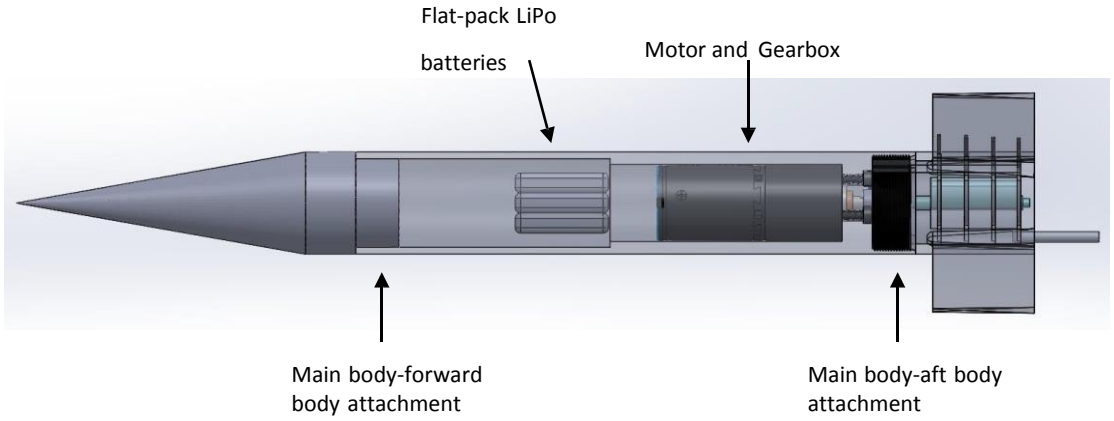

Figure 20. CAD Side View of Integrated Projectile.

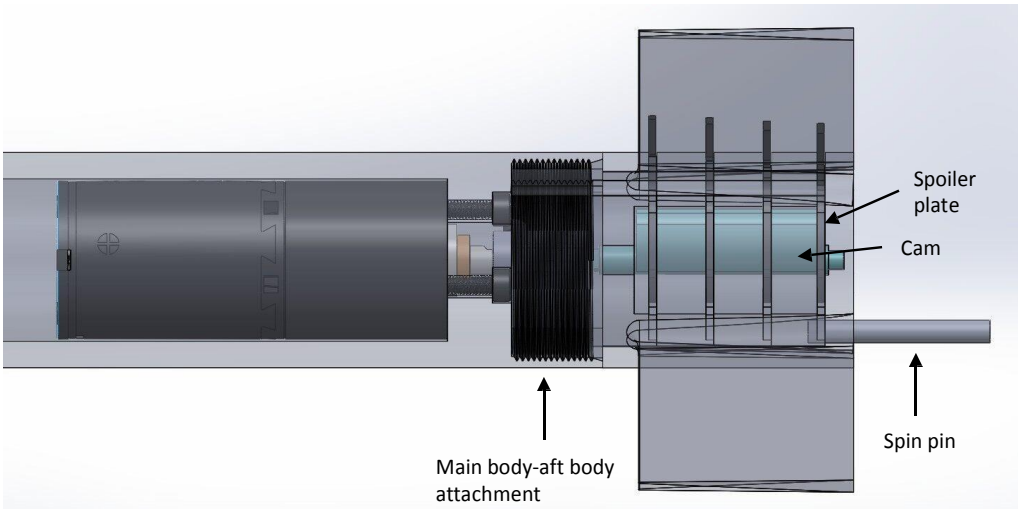

Figure 21. CAD Side View of Integrated Projectile (Rear Zoom).

Figure 22. Maxon A-max 110147 Brushed DC Motor (left). Maxon A-max Motor Attached to ARL Shock Table (right).

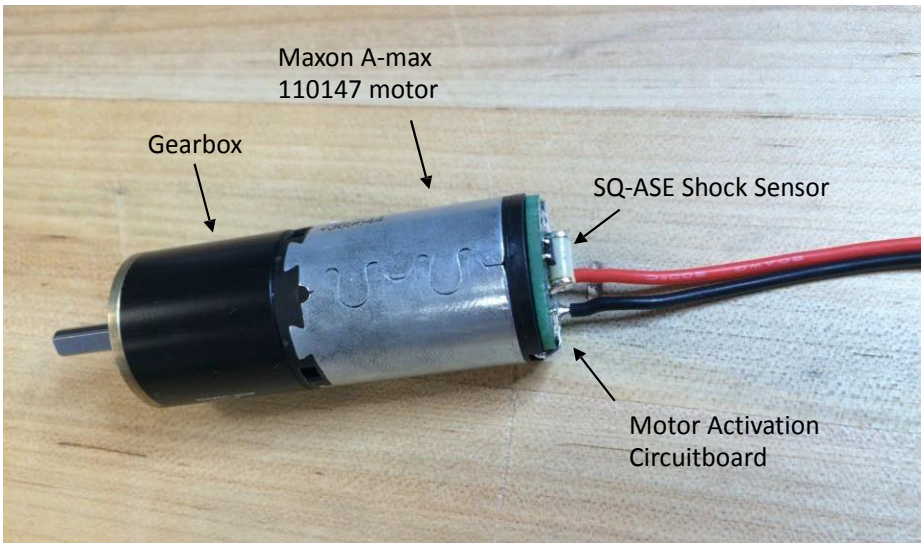

Figure 23. Motor Activation Latching Circuit PCB Assembly with Integrated Shock Switch.

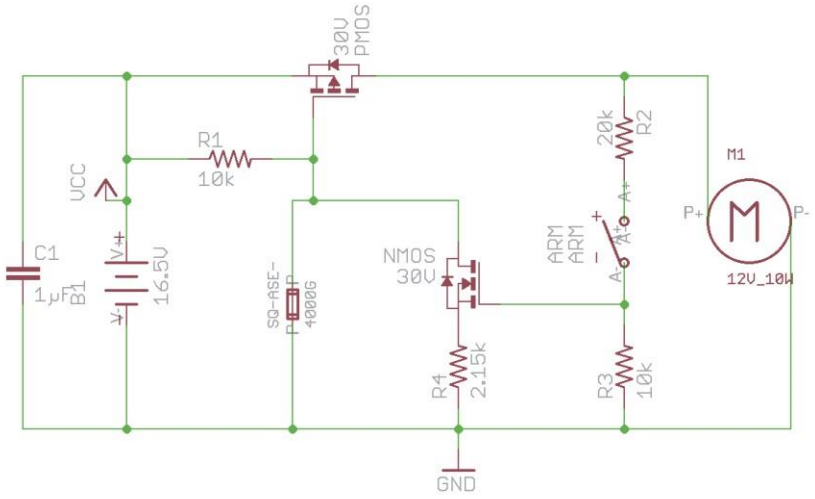

Figure 24. Latch Circuit Schematic Used in Microspoiler Projectile Flight Experiments.

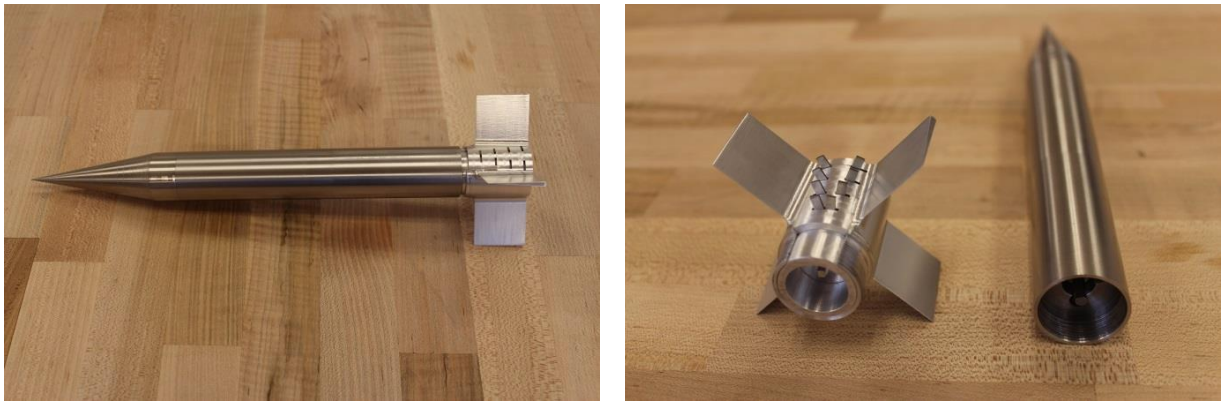

Figure 25. Fully Integrated Projectile Prototype Including Active Microspoiler Mechanism.

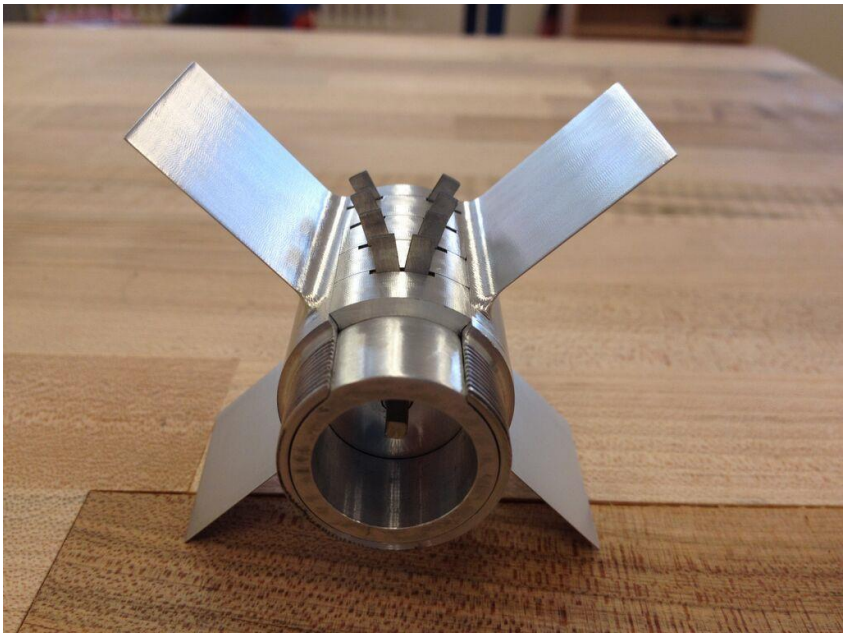

Figure 26. Fully Assembled Active Microspoiler Assembly in Aft Section of Projectile.

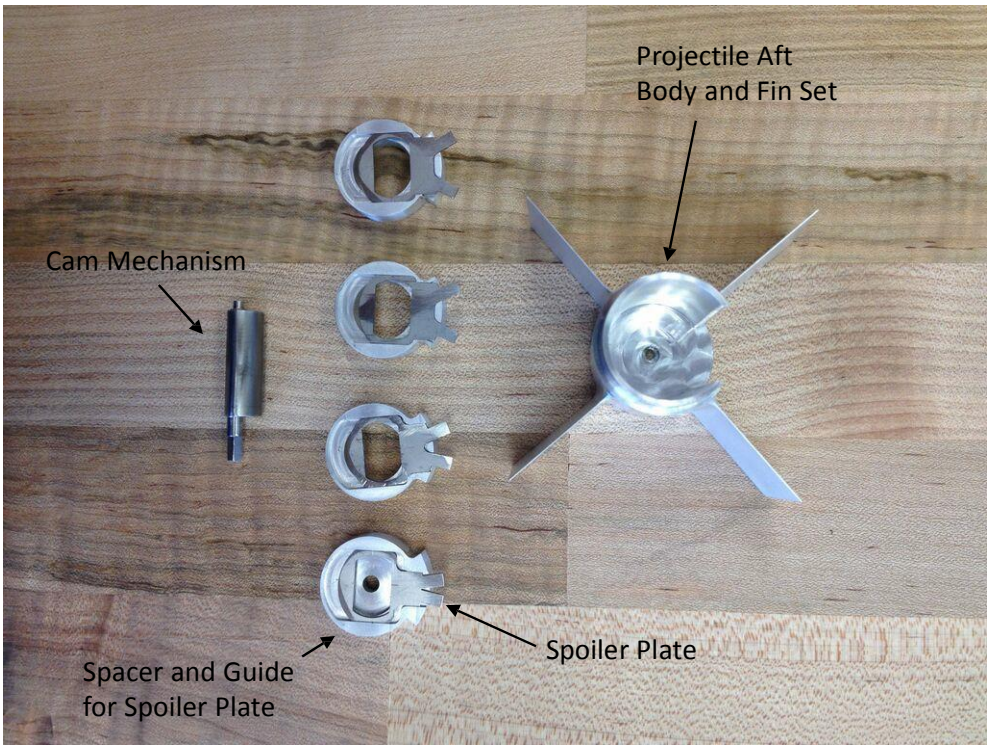

Figure 27. Components of the Active Microspoiler Assembly.

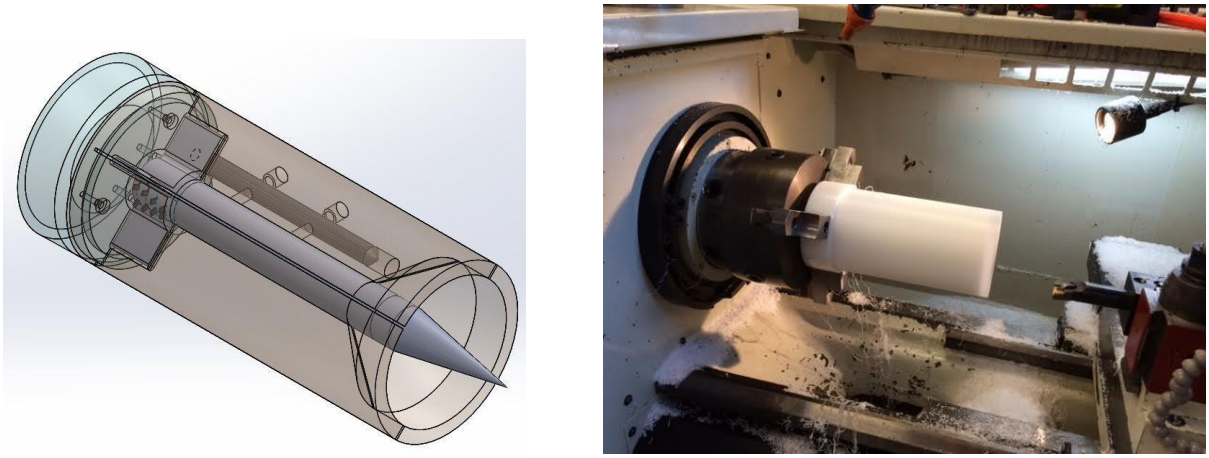

Figure 28. CAD Model of Integrated Projectile-Sabot Assembly (left), Sabot Fabrication at Georgia Tech Machine Shop (right).

G. Special Comments

None.

H. Implications for Further Research

In light of the results presented above, this project successfully achieved all the specified program goals. One immediate possibility for future research is to further improve the mechanical and electrical design and perform a divert test. The purpose of this test would be to characterize experimentally the maximum divert capability of the mechanism at a given launch configuration. This lateral acceleration value can then be compared to predictions from this project, and extrapolated to other rounds and launch conditions. Such a test would require the prototype projectile design to be modified to include a roll-angle sensor and digital microprocessor. Given Georgia Tech's experience during this project, a divert test can likely be conducted within approximately 12 months.

Another possible idea for future research is to explore more extensively applicability of the mechanism to spin-stabilized projectiles. Currently, the effect of high spin rates on performance of the mechanism are not completely known. Furthermore, it is not immediately clear how to implement such a mechanism mechanically onboard a spin-stabilized round, and how much the current design could be leveraged. Thus, a potential future project would be to perform additional CFD studies at high spin rates, and implement a prototype microspoiler actuator on a large-caliber or medium-caliber spinner.

A final possibility for future research would be to further explore the potential to combine microspoiler and canard actuators on the same round. Possible interference effects between the canards and spoilers should be characterized in CFD (obviously this effect depends on relative placements of the actuators). Furthermore, a prototype projectile could be built demonstrating feasibility of implementing both actuators on the same projectile, which may be somewhat complicated mechanically. It is likely that such a prototype implementation could leverage the current mechanical design substantially.

The views, opinions and/or findings expressed are those of the author and should not be interpreted as representing the official views of the Department of Defense or the U.S. Government.